Surface coatings of silver nanowires lead to effective, high conductivity, high-strain, ultrathin sensors

Conor S Boland[1]*, Umar Khan[2], Hanane Benameur[1] and Jonathan N Coleman[1]*

[1]*School of Physics, CRANN and AMBER, Trinity College Dublin, Dublin 2, Ireland*

[2]*Department of Life Sciences, PEM Centre, School of Science, Sligo Institute of Technology, Sligo Ash Lane, Sligo, Ireland*

*bolandc1@tcd.ie & colemaj@tcd.ie

Abstract:

Integrated sensors for bodily measurements require a sensing material that are highly conductive, flexible, thin and sensitive. It is important that these materials be non-invasive in application but robust in nature to allow for effective, continuous measurement. Herein, we report a comparative study of two simple, scalable methods to produce silver nanowire (AgNW) polyurethane (PU) composite materials: layer-by-layer (LBL) and mixed filtration. Both types of composites formed were ultrathin (~50 μm) and highly conductive (10^4 S/m), with the LBL method ultimately found to be superior due to its low percolation threshold. Electrical resistance of the LBL composites was found to vary with strain, making these materials suitable for strain sensing. LBL composites displayed a working strain up to ~250% and a high gauge factor (*G*), with values of *G*~70 reported. The sensors reported here were ~10^9 –times more conductive and ~10^4 –times thinner than their carbon-based composite sensor counterparts with similar gauge factor. This made the strain sensors presented here among one of the most flexible, highly sensitive, thinnest, conductive materials in literature. We demonstrated that with these properties, the LBL composites formed were ideal for bodily motion detection.

Introduction:

Of late, smart technologies have become seamlessly integrated into society, and with that, its influence becomes more profound in our daily lives. In an age of continuous, fast

data transfer via media and communication devices, it is no surprise that smart technologies have started to trend towards medical applications.[1] Supplying us with up-to-date information about our own bodies through medical devices in a wearable form has become an exciting area in research and development.[1, 2] To realise these wearable medical sensors, measurement components capable of undergoing varying degrees of reversible deformation during dynamic motions are required. These materials must also be highly conductive, lightweight and discrete.[3-5] Due to their rigid nature, commercially available silicon-based materials are unsuitable for such applications. However, recently flexible, low stiffness, highly sensitive, cost-efficient sensors made from polymer based nanocomposites have been shown to be ideal for use in next generation wearable smart materials and flexible electronics.[6-8]

Nanocomposite sensing materials consisting of an elastic polymer matrix loaded with conductive carbon-based nanomaterials[9-22] have been utilized to try and meet the above criteria. In such nanocomposites, when strain is applied the distance between conductive fillers inside the polymer matrix changes, causing large resistive changes, resulting in sensitivities much larger than that of commercial strain sensors. This strain-dependent resistive change of the composites at small deformations (<1% strain) can be described by:

$$\Delta R / R_0 = G\varepsilon \quad (1)$$

This expression relates the fractional resistance change ($\Delta R / R_0$) of the composite to the strain (ε) by a sensitivity metric known as the gauge factor (*G*). For commercial silicon strain sensors, the gauge factor is ~2 with a working strain range of < 10%.[23] For nanocomposites however, working strains as high as 800%[17] and values of $G \sim 1000$[21, 24] have been reported. With their pliable nature and high *G* values, in application, these nanocomposite sensing materials have been demonstrated as highly effective bodily sensors.[17, 21]

It is commonly known that around the electrical percolation threshold, the value of *G* for most nanocomposites is at its highest.[17, 21] Conversely and consequently, at this point the conductivity of the material is generally very low ($\leq 10^{-5}$ S/m, Table S2) for these carbon-based nanocomposites. With such low conductivities, the power supply options are limited to bulky lab-based setups; hindering the progression toward the realisation of commercial, wireless, discreet wearable electronics made from these materials. . As an alternative material, silver nanowires (AgNWs) have been of great interest[25-38] due to the ability to

form highly conductive percolative networks.[38-41] AgNW based sensing composite materials, formed exclusively by layer deposition, consist of a percolative network of the nanowires adhered to a flexible polymer substrate. Similar to carbon nanotube (CNT) buckypaper composites[42-44], adhesion to the polymer base gives the low-density network structure and allows for reversible elastic deformation. AgNW composites produced by layer deposition have displayed *G* values as large as 90[27] and working strains as high as 220%.[37] However, no AgNW composite has reported both high working strain (>100%) simultaneously with high gauge factor ($G > 20$) (see SI, Table S1). Nor has a mixed composite (the most common form of carbon based sensing composite), using AgNWs as fillers, been investigated for comparative studies. In this work, we compare and characterise AgNW:PU composites prepared using a layer by layer method[45] and mixing filtration to form conductive composites. Furthermore, we demonstrate that the composite materials formed were thin, highly conductive, work at high strains and possess large gauge factors ideal for sensitive bodily monitoring.

Results and Discussion:

Composite Preparation

To prepare the LBL and mixed composite samples (Fig 1), water-based AgNW and PU dispersions were purchased from suppliers. From SEM images of the nanowires deposited on a PET membrane (Fig. 2A), the AgNWs used for formation of both composite types were seen to have large aspect ratios. All visible nanowires appeared greater than ~3μm in length. Histograms in Fig. 2B, show the number count of the diameters (top) and lengths (bottom) of the AgNWs found in the dispersion after 5 mins of bath sonication. From the statistical SEM, we found the mean diameter and lengths of the nanowires to be ~ 69 nm and ~ 7 μm respectively.

For forming the LBL composites (Fig 1A), AgNW dispersions of varied concentration were split into two fractions. The first fraction was filtered on to a PET membrane after which the polymer solution followed, coating one side of the AgNW paper, followed by the remaining AgNW dispersion. This yielded an ultrathin (~50 μm), robust, free-standing composite with an AgNW:PU:AgNW sandwich structure which transitioned from translucent grey to metallic silver in hue with increasing AgNW mass fraction. (see Fig. 2C). In this case,

mass fraction (M_f) varied between 0.1% and 20%, with the quoted mass fractions describing the AgNW content on both sides of the composite combined. Looking at an SEM image of the freeze fracture cross section of a M_f ~ 8% LBL composite (Fig. 2D), the AgNW layers that sandwiches the polymer layer can be seen (inset).

For the formation of the mixed composites (Fig 1B), dispersions with varied concentration of AgNWs were added to PU dispersions. All composite solutions contained a constant mass of AgNWs and PU to produce solutions with mass fractions that varied between 0.1% and 20%. The AgNW:PU mixtures were then vacuum filtered onto a PET membrane to again produce an ultrathin (~50 um), free-standing, circular composite which transitioned from translucent grey to metallic silver in hue with increasing filler loading levels (see Fig 2C). In Fig. 2E, an SEM image of the surface of a M_f ~ 8% mixed composite can be seen. Looking at the inset in the figure, AgNWs wrapped in polymer can be seen to be protruding from the surface of the composite.

Composite Electrical Properties

For each composite preparation method, electrical conductivity (σ) was measured as a function of mass fraction. In Fig. 3A, conductivity was seen to increase with mass fraction in both composite types, from $\sigma \sim 10^{-6}$ S/m at M_f ~ 0.1% to $\sigma \sim 10^{4}$ S/m at M_f ~ 8%. It can be noted that the LBL composite required a much lower mass fraction of AgNWs (M_f ~ 0.4%) to start to conduct an appreciable amount of current compared to the mixed sample which required a much higher AgNW content (M_f ~ 5%). We would expect a lower threshold for conduction in the LBL sample due to the localisation of the nanowires in a high-density network on the composite surface.

For a composite consisting of a 2-D network of 1-D conductive rods laying on top of an insulating polymer layer, the electrical conductivity of the network can be described by percolation theory.[46] Current flow in such a system is dependent on the loading level being above a critical network density (rods per unit area, N) known as the percolation threshold, N_c. This figure describes a network density where the first continuous conductive pathway across the network forms. For a composite where $N > N_c$, the conductivity of the system is described by the percolation scaling law[46]:

$$\sigma = \sigma_0 (N - N_c)^{t_{2D}} \quad (2)$$

Where σ_0 is a constant and t_{2D} is the percolation exponent.[46, 47] Fitting Eq. 2 to the conductivity data of the LBL composite in Fig. 3B, the value for the critical density is found to be N_c ~ 0.5 μm^{-2} (Fig 3C). From the fit in Fig 3C, a value of t_{2D} ~ 1.41 is found to be in good agreement with data. The value for *t* here is in good agreement with the expected value of ~1.3 for a 2-D system.[46]

In a 3-D composite consisting of a mixture of conducting rods in a polymer matrix, the rods tend to be randomly dispersed throughout a matrix, leading to a slightly differnet percolation scaling law which depends on the filler volume fraction, ϕ: $\sigma = \sigma_0 (\phi - \phi_c)^{t_{3D}}$. In 3-D, the percolation threshold can be shown to scale with the aspect ratio of the filler as[48]:

$$\phi_c = 0.6D / L \quad (3)$$

where *D* is the filler diameter and *L* is the filler length. Using the SEM statistics from Fig. 2B and Eq. 3, a value of $\phi_{c,Theory}$ ~ 0.59% is expected for a mixed composite with a 3-D network of AgNWs from this work. Looking at the conductivity as a function of volume fraction for the mixed samples in Fig. 3D, conductivity is seen to dramatically jump in value at ϕ_c ~ 0.5%, from σ ~ 10^{-6} S/m to σ ~ 10^4 S/m, which correlates to the theoretical value predicted by SEM for the first conductive pathway to form. The percolation threshold values reported here in this work were found to be in good agreement with other values calculated in literature for both layered[49] and mixed[50] composites using AgNWs of similar dimensions. From the electrical characterisation, it is very much apparent that the LBL method of composite production is superior to its mixed composite counterpart due to its much lower percolation threshold.

Mechanical characterisation and Electromechanical Response

As previously discussed, the addition of the AgNWs onto either side of the insulating PU matrix's surface resulted in electrically conductive composites. From mechanical tests in Fig S1&2, the LBL composites demonstrated high strain at break (>400%) and low moduli (>100MPa), which would make these composites ideal for application as strain sensors. For the LBL samples, during electromechanical testing (Fig. 4A), electrical resistance increased

upon the application of strain. This increase in resistance is due to the deformation of the network under strain. The resistance is found to increase with strain up to >200% (see SI, Fig. S3), with resistance becoming immeasurably at strains past these values. It should be noted this is not due to fracture of the composites or degradation, but the rarefication of the conductive network beyond the percolation point with further increasing strain.

The fractional resistance change ($\Delta R / R_0$) versus strain on a log-log plot was found to scale approximately linearly at low strain (<1%) in accordance with Eq. 1 (Fig. 4B). The slight nonlinearity at low strain noted here, is not uncommon in strain sensing composites synthesised through the layer deposition method. Such nonlinearity has been reported in a wide variety of deposited materials, such as CNTs,[51, 52] graphene,[53, 54] and AgNWs.[55] These non-linearity's are thought to be due to non-uniformity of the deposited conductive layer leading to areas of high and low densities. These density differences in the layer cause uneven stress transfer between the network and the substrate, leading to necking in the network during deformation.[28]

Fitting Eq. 1 to all curves (see SI, Fig S4), allowed for the calculation of gauge factor (G). Plotting the respective values of G as a function of mass fraction in Fig 4C, values are found to steadily increased with mass fraction up to M_f ~ 12% and a value of G ~70. This is contrary to what has been reported in most composite sensing materials, where G is seen to decrease with network density[28] and loading levels.[21] However, similar trends in G have been reported in mixed CNT[56, 57] and graphene composites,[19] as well as layered CNT[58] and patterned polysilicon composites.[59] This increase in sensitivity with M_f (i.e. network density) present here, draws parallel with highly connective CNT thin films which also display a similar trend.[60] Naturally, the conductivity, and thus the number of CNT-CNT junctions, are seen to scale with overall network density. The said conductivity of the films were found to be very highly dependent on the number of junctions present. Thus, as strain is applied to such a network, the number of junctions would change as the network deformed. This gives rise to the large resistive changes, and thus the high sensitivities, seen in layer deposition composite sensors.[58, 60] The findings from these quoted works, and the work presented here, alludes to the mechanism behind the large resistive changes seen in layer deposition composites being much more complex than the simple assumption of just interconductor distance change. Increasing M_f (>12%) further, gauge factor is found to

decrease to G ~ 30 (Fig. 4C). This, however, can be explained by the very large increase in composite stiffness (see SI, Fig. S2) resulting in lessened layer deformation with strain.

From literature, in Fig. 4D-F, the values for gauge factor, strain, conductivity, and thickness displayed by the LBL composite are seen to be among the highest (see SI, Table S1&2). In comparison to commercial stain sensors, all values of G here were higher than the industry standard of G ~2. Looking at literary values of gauge factor as a function of strain (Fig. 4D), the LBL composite strained further and was more sensitive than most carbon composite sensors types, as well as other Ag-based composites. For Ag-based composites with similar working strains, the LBL composite was found to be ~3-times more sensitive. Plotting gauge factor versus conductivity in Fig. 4E, the LBL composite is found to again outperform others. For carbon-based composites with a similar gauge factor, the sensors reported here were ~10^9 –times more conductive. Looking at the gauge factor as a function of composite thickness in literature (Fig 4F), the LBL composite is found to be one of the thinnest sensing materials and is ~5-times and ~10^4 -times thinner than Ag and carbon composites that display similar gauge factor, respectively.

The LBL AgNW:PU composite sensor is among one of the most conductive, stretchable, thinnest, highly sensitive materials in literature. To test response repeatability and durability, a 12% LBL sample was tested under a step-strain profile. Under these conditions the LBL strip was held at various strains from 0% to 70%, in increasing increments of 10% strain, for 60s per increment. Plotting the strain and electrical profiles as a function of time in Fig. 5A, both are seen to match each other in shape closely. In particular, looking at the increasing and decreasing increment sides of the resistance trace, both are seen to mirror one another. It is also noticed that at each increment of strain the resistance of the composite remains constant, with no sign of decay with time. Looking at dynamic response of the composites, two LBL samples (1% and 20%) were tested using a tensile tester under a cyclic strain profile at a frequency of 0.33 Hz. The profile was trapezoidal in shape with the minimum strain of the profile being 5% and the maximum strain being 20% (Fig. 5B&C). For both the 1% (Fig. 5B) and the 20% (Fig. 5C) samples, the resistance followed the strain trace quite accurately, with no degradation in response noted during the 500 cycles. However it can be noted that the 20% sample underwent some conditioning during initial cycling (first ~100 cycles), after which its response was constant. This is consistent with previous work on graphene/rubber composite sensors[17] which presented similar conditioning behaviour.

Applications

With the LBL composites sustainable high-performance metrics and elastic nature, we believe these composites would make excellent candidates for bodily sensing. Ideally for real application, these materials would be encapsulated to protect the sensing materials performance from decay due to wear and tear and to protect the user from agitation that could arise from material on skin contact. Though encapsulation was not performed on the materials presented here, we are still able to show a proof of concept of these composites in application as bodily sensors with no hindrance in performance or measurement noted. All application tests were performed by measuring the sample with highest value of gauge factor (12% LBL sample) electrical response, in resistance as a function of time, to bodily stimuli. A strip of the 12% sample was attached across the first knuckle (Fig 6A) of the index finger. The resistance verse time trace (Fig. 6B) was found to increase with bending and decrease with subsequent straightening of the finger, undergoing strains up to ~50%. The composite sensing material was seen to follow the movement of the joint accurately and at different rates of bending. In Fig 6C, the LBL strip stretched (~20% strain) across the Achilles heel of the subject. In Fig. 6D, as the subject rocked up and down on their toes the strain on the strip went through cycles of relaxation and tightening, resulting in a resistance decrease and increase. To demonstrate the composite's ability to be integrated into a simple circuit, a 12% LBL strip was placed in series with a 4xAA battery pack and an LED light (Fig 6E). Due to the composites high conductivity, the LED's ability to light was not impeded by the presence of the LBL strip in the circuit. When the strip is stretched, the LED dims. Upon the release of the strip, it returns to its unstrained state, and the LED returns to its original brightness.

Conclusions

In this work we demonstrated two simple, scalable methods for producing AgNW composites through layer-by-layer (LBL) filtration and mixed filtration. The introduction of the nanowires resulted in composites that were conductive, with percolation thresholds of N_c ~ 0.5 μm^{-2} and ϕ_c ~ 0.5% observed for LBL and mixed samples, respectively. The composites' resistances were found to be strongly dependent on strain during electromechanical testing, making them strain sensors. Gauge factors up to G ~70 and large working strains (>200%) were reported for the LBL composite. Compared to other composite

sensing materials, the LBL was ~3 -times more sensitive and ~5 -times thinner than Ag-based composites with similar working strains and ~10^9 –times more conductive and ~10^4 -times thinner than carbon-based composites with a similar gauge factor. With such high conductivity, sensitivity, and elasticity displayed by the LBL composites, we were able to fully display the sensing materials application as a bodily sensor.

Methods:

Materials for Composites: A stock Polyurethane (PU)/water dispersion Hydrosize U2022 (1g/mL) used in this work was provided by Michelman Inc. The Silver Nanowires (AgNWs) stock solution was a AW060 AgNWs:water solution (10 mg/mL concentration, average diameter <D> = 55~75 nm, average length <L> = 10~20 um) purchased from Zhejiang Kechuang Advanced Materials Technology Co., Ltd. For filtration and composite production, Sterlitech PET filter membranes pore size 0.45 microns were used.

Composite Production: AgNW:PU composites of various mass fractions were made by two methods; 1) layer by layer (LBL) vacuum filtrations and 2) mixed filtration. In both cases the total mass of the composites were kept constant (80mg). The total volumes of AgNWs:water and PU:water dispersions were kept constant through dilution with water, i.e 10 mL and 50 mL respectively.

Layer by layer filtration: For each mass fraction sample the AgNW dispersion was split into two fractions, each 5mL in volume and 10 mL in total volume. One fraction of the AgNW dispersion was sonicated in a low power sonic bath for 5 minutes. It was vacuum filtered onto the PET membrane. As soon as the AgNWs:water filtration was finished, 50 mL of PU/water was poured on top and filtered. Once the water had filtered through, the system was left under vacuum for a further 5 minutes during which the second fraction of AgNWs:water was prepared by bath sonication for 5 minutes. This fraction was then poured in on top of the AgNW:PU paper and filtered. The composite was then left under vacuum for 5 Hrs. This yielded a final composite with an AgNW:PU:AgNW sandwich structure which was further dried at 60 °C overnight (~14 Hrs) in an oven.

Mixing filtration: For each mass fraction PU (50mL) and 10 mL of AgNWs was mixed and sonicated using a sonic bath for 5 minutes. The different mass fraction AgNW:PU dispersions

were then filtered on PET membranes. The composite papers were then left under vacuum for 5 Hrs and further dried at 60 °C overnight (~14 Hrs) in an oven.

Characterisation: All the films were cut into strips 20mm in length and 2.25 mm in width. The bulk conductivity was measured using the four-probe technique with silver electrodes of dimensions and spacings of typically ~ millimetre size and a Keithley 2400 source metre. Electro-mechanical measurements were performed using a Keithley KE2601 source meter in 2-probe mode, controlled by LabView software, in conjunction with a Zwick Z0.5 ProLine Tensile Tester (100 N Load Cell). Samples were tested at a strain rate of 5 mm/min with a constant gauge length of 9 mm. Mechanical and electromechanical response values reported here are the mean of five tested sample strips per mass fraction with corresponding standard error. Scanning electron microscopy (SEM) was performed using a Zeiss Ultra Plus Field Emission Scanning Electron Microscope. Using the SE2 lens, samples were examined at a working distance of ~5 mm, with a 30 μm aperture and 5 keV beam strength.

Application Testing: Informed consent was obtained from the subject for the testing. All application tests were performed by measuring a 12% sample's electrical response, in resistance as a function of time, to bodily stimuli using a Keithley KE2601 source meter. For the finger response test, the strip (attached to the source meter via silver wire) was taped across the first knuckle of the index finger. For the heel response, the strip was stretched across the Achilles heel of the subject. The change in resistance while the subject bounced on their toes was measured as a function of time, again by attaching the strip to the source meter via silver wire.

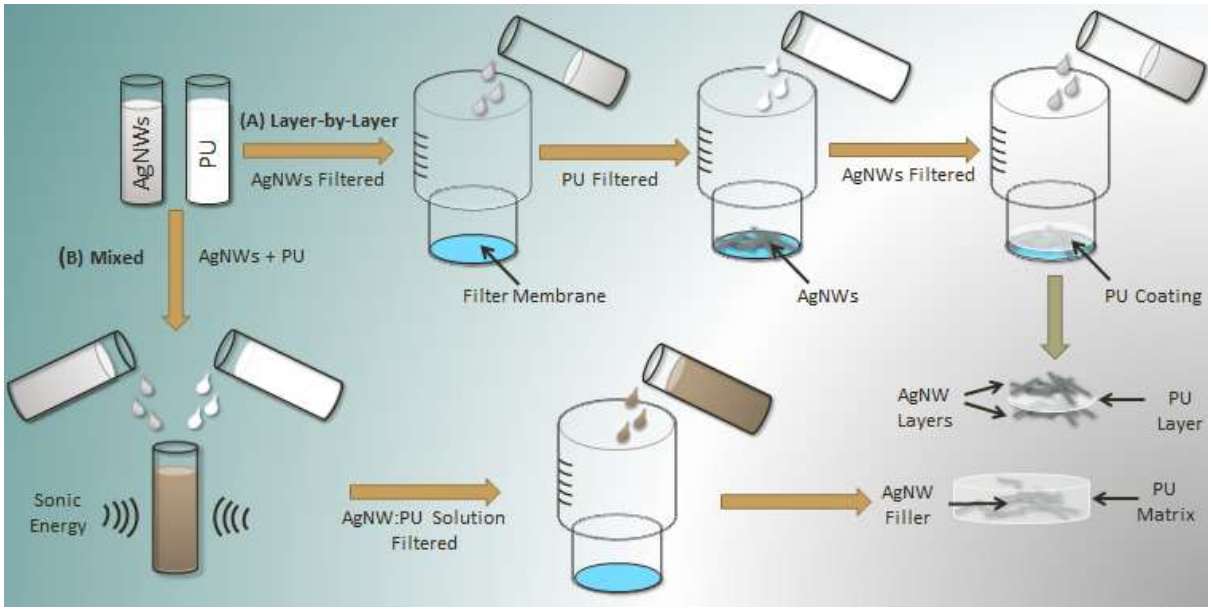

Figure 1: Scheme of A) Layer-by-Layer and B) Mixed methods of AgNW:PU composite production.

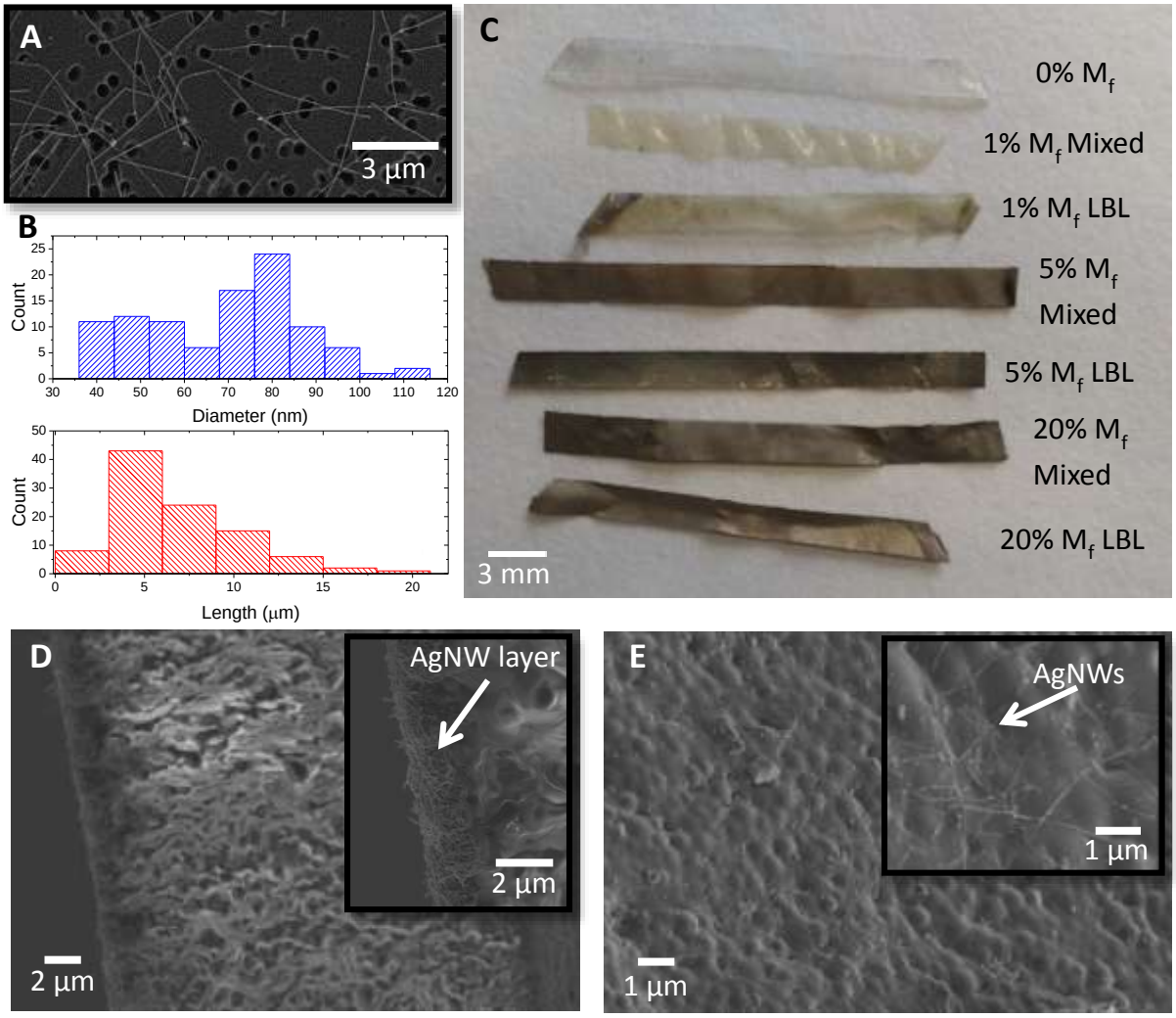

Figure 2: Characterisation of AgNWs and composites. A) SEM image of AgNWs. B) Histograms of dimeter (top) and length (bottom) counts taken from SEM images of the silver wires. Mean diameter and length was found to be 68.69 nm and 6.929 µm, respectively. C) Image of LBL and mixed composite strips ranging from M_f=0% to M_f=20%. D). SEM image of LBL M_f ~ 8% AgNW:PU composite. This involved an AgNW layer deposited either side of the polymer substrate (inset). E) SEM image of mixed M_f ~ 8% AgNW:PU composite. Nanowires coated in polymer are seen to be protruding out of the surface of the composite (inset)

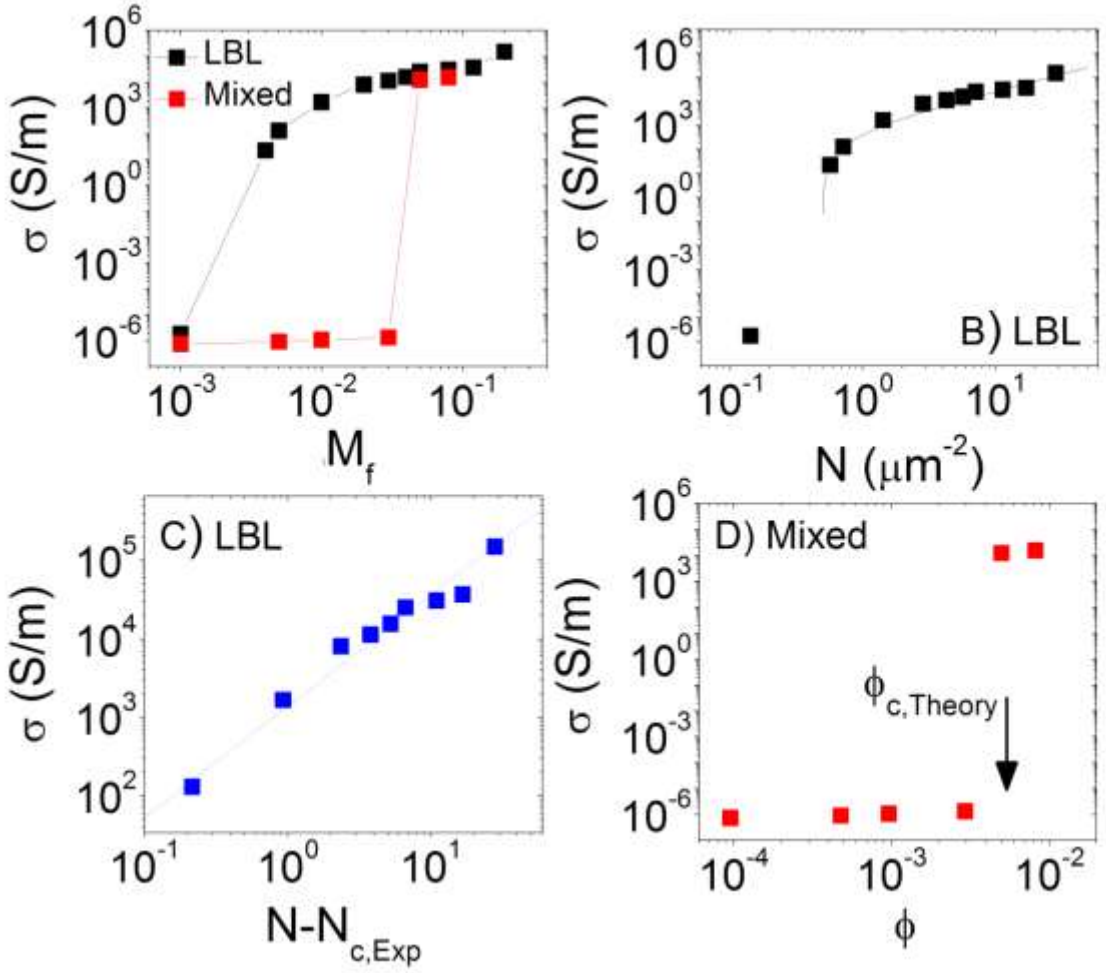

Figure 3: A) Conductivity versus AgNW mass fraction for PU-based composites prepared both by layer by layer and mixing technique. B) Conductivity versus number density of AgNWs on the PU surface. The solid line is a percolation fit using equation 3 described by a critical density of N_c ~ 0.5 μm^{-2} and an exponent t ~ 1.41. C) Conductivity verse reduced nanowire number density. Dashed line is a fit to Eq 3. D) Conductivity versus volume fraction for mixed composites. The arrow shows the theoretical percolation threshold (ϕ_c ~ 0.59%) as calculated from equation 2 using SEM statistics from Fig 2B.

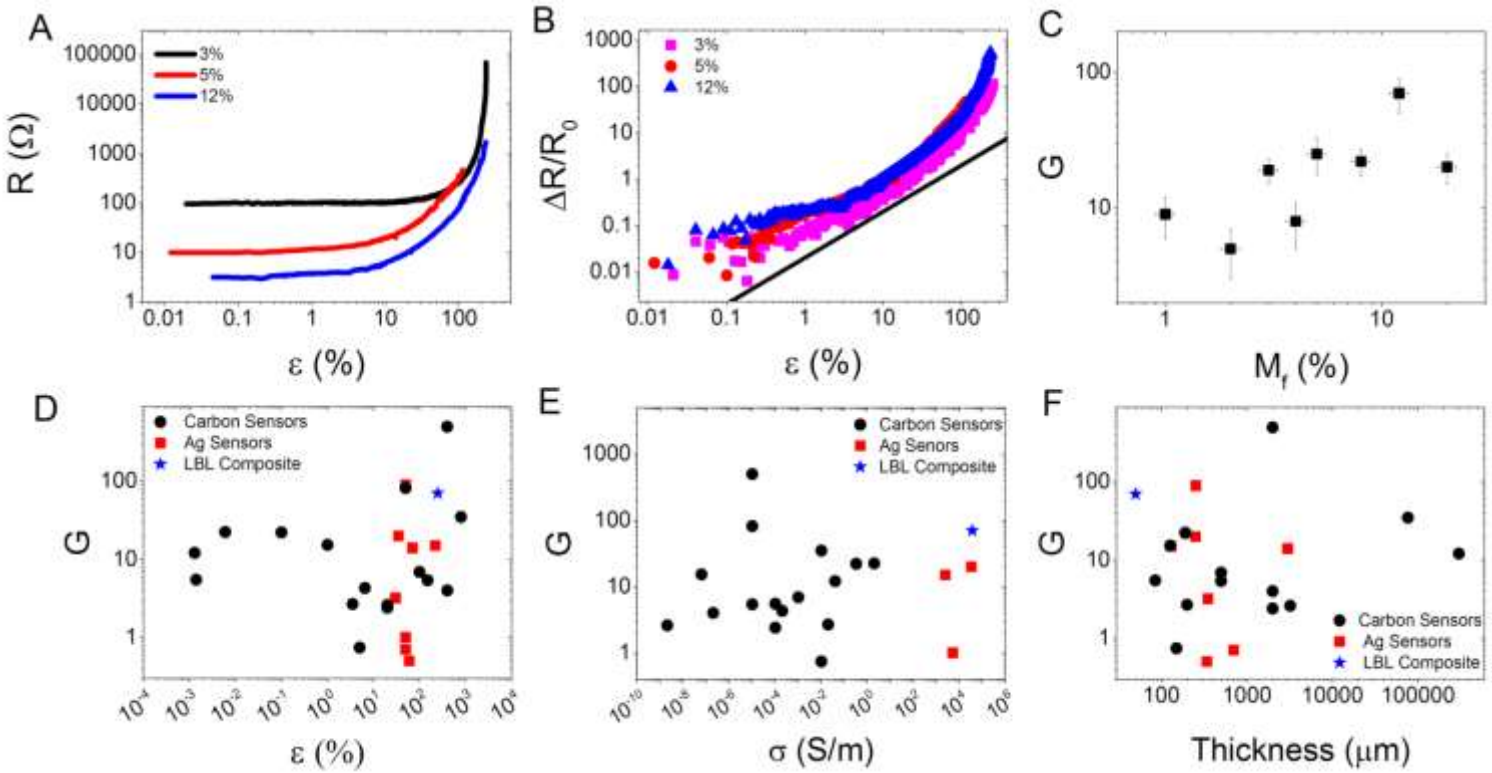

Figure 4: Mechanical and Electromechanical Characterisation. A) Resistance measured as a function of applied strain for M_f ~ 3%, 5% and 12% samples. B) Fractional resistance change ($\Delta R / R_0$) of composites as a function of strain. Solid line is a fit for Eq. 1 with a value of gauge factor being G ~ 2, representative of a commercial strains sensor. C) Gauge Factor (G) values calculated from Eq. 1 and extracted from B and Fig. S4 plotted as a function of M_f. D-F) Summary of results reported in the literature for nanocomposite strain sensors against results reported in this work. D) Maximum reported gauge factor versus maximum reported strain (see SI, Table S1&2). E) Maximum gauge factor in literature as a function of maximum conductivity (see SI, Table S1&2). F) Maximum gauge factor versus composite thickness. In all cases (E-F), the LBL sample is found to be among the best values for each metric.

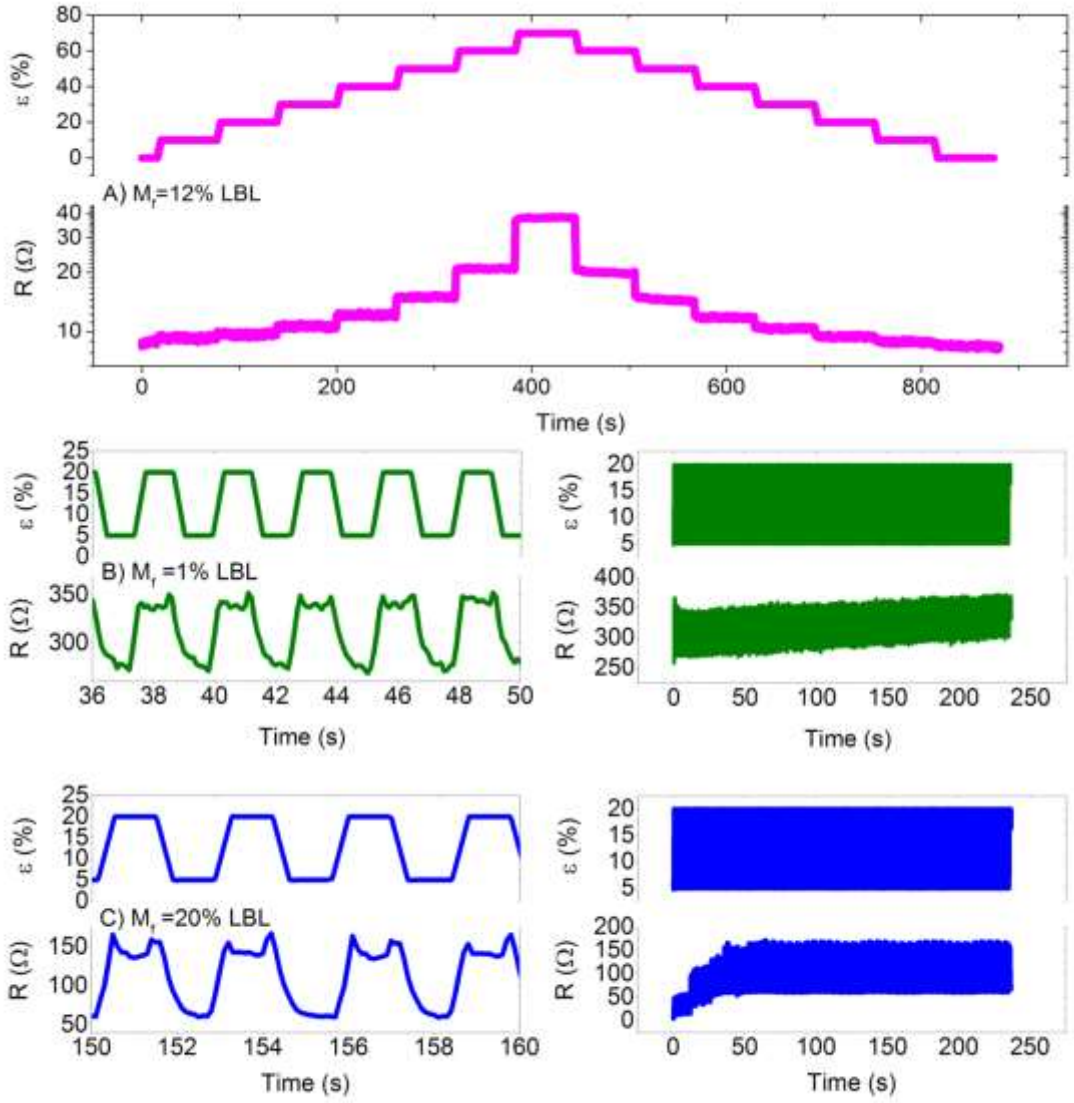

Figure 5: A) Step-strain testing of 12% LBL composite held at strains for 60s in increasing and decreasing increments of strain from 0-70%. Cyclic testing of composites with data for B) a 1% LBL composite and C) a 20% LBL composite over 500 cycles at 0.33 Hz.

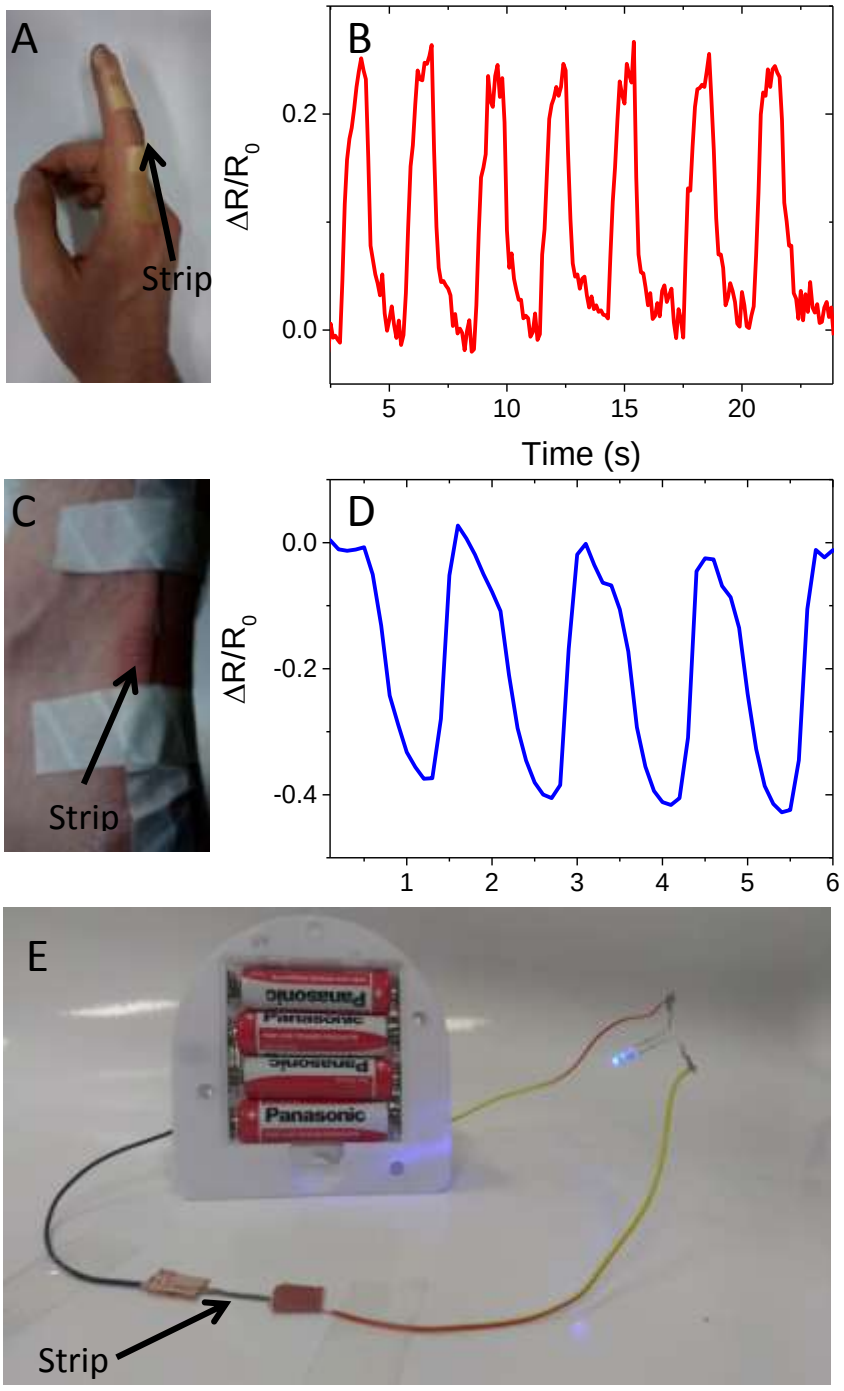

Figure 6: Application Testing. Electrical response to bodily stimuli: M_f ~ 12% LBL AgNW:PU composite strip while attached to A-B) the index finger and across C-D) the Achilles heel of the subject. E) M_f ~ 12% LBL AgNW:PU composite strip powered by AA battery pack in series with LED light.

References

1. Gong, S. and W. Cheng, *One-Dimensional Nanomaterials for Soft Electronics.* Advanced Electronic Materials, 2017. **3**(3): p. n/a-n/a.
2. Amjadi, M., et al., *Stretchable, Skin-Mountable, and Wearable Strain Sensors and Their Potential Applications: A Review.* Advanced Functional Materials, 2016. **26**(11): p. 1678-1698.
3. Rogers, J.A., T. Someya, and Y. Huang, *Materials and Mechanics for Stretchable Electronics.* **327**(5973): p. 1603-1607.
4. Pantelopoulos, A. and N.G. Bourbakis, *A Survey on Wearable Sensor-Based Systems for Health Monitoring and Prognosis.* **40**(1): p. 1-12.
5. Kaltenbrunner, M., et al., *An ultra-lightweight design for imperceptible plastic electronics.* **499**(7459): p. 458-463.
6. Gaddam, A., et al. *Wireless Sensors Networks based monitoring: Review, challenges and implementation issues*. in *3rd International Conference on Sensing Technology, 2008. ICST 2008*. 2008.
7. Bandodkar, A.J. and J. Wang, *Non-invasive wearable electrochemical sensors: a review.* Trends in Biotechnology, 2014. **32**(7): p. 363-371.
8. Windmiller, J.R. and J. Wang, *Wearable Electrochemical Sensors and Biosensors: A Review.* Electroanalysis, 2013. **25**(1): p. 29-46.
9. Park, M., et al., *Highly stretchable electric circuits from a composite material of silver nanoparticles and elastomeric fibres.* Nature Nanotechnology, 2012. **7**(12): p. 803-809.
10. Alamusi, et al., *Piezoresistive Strain Sensors Made from Carbon Nanotubes Based Polymer Nanocomposites.* Sensors, 2011. **11**(11): p. 10691-10723.
11. Hu, N., et al., *Investigation on sensitivity of a polymer/carbon nanotube composite strain sensor.* Carbon, 2010. **48**(3): p. 680-687.
12. Hu, N., et al., *Tunneling effect in a polymer/carbon nanotube nanocomposite strain sensor.* Acta Materialia, 2008. **56**(13): p. 2929-2936.
13. Pham, G.T., et al., *Processing and modeling of conductive thermoplastic/carbon nanotube films for strain sensing.* **39**(1): p. 209-216.
14. Pham, G.T., et al. *Nanotailored thermoplastic/carbon nanotube composite strain sensor*. 2006.
15. Yin, G., et al., *A carbon nanotube/polymer strain sensor with linear and anti-symmetric piezoresistivity.* Journal of Composite Materials, 2011. **45**(12): p. 1315-1323.
16. Zhang, W., J. Suhr, and N. Koratkar, *Carbon nanotube/polycarbonate composites as multifunctional strain sensors.* Journal of Nanoscience and Nanotechnology, 2006. **6**(4): p. 960-964.
17. Boland, C.S., et al., *Sensitive, High-Strain, High-Rate Bodily Motion Sensors Based on Graphene–Rubber Composites.* ACS Nano, 2014. **8**(9): p. 8819-8830.
18. Kim, Y.-J., et al., *Preparation of piezoresistive nano smart hybrid material based on graphene.* Current Applied Physics, 2011. **11**(1, Supplement): p. S350-S352.
19. Eswaraiah, V., K. Balasubramaniam, and S. Ramaprabhu, *One-pot synthesis of conducting graphene–polymer composites and their strain sensing application.* Nanoscale, 2012. **4**(4): p. 1258-1262.
20. Eswaraiah, V., K. Balasubramaniam, and S. Ramaprabhu, *Functionalized graphene reinforced thermoplastic nanocomposites as strain sensors in structural health monitoring.* Journal of Materials Chemistry, 2011. **21**(34): p. 12626-12628.
21. Boland, C.S., et al., *Sensitive electromechanical sensors using viscoelastic graphene-polymer nanocomposites.* Science, 2016. **354**(6317): p. 1257.
22. Paleo, A.J., et al., *The piezoresistive effect in polypropylene-carbon nanofibre composites obtained by shear extrusion.* **19**(6): p. 065013-065013.

23. Window, A.L., *Strain Gauge Technology*. 1992.
24. Kost, J., M. Narkis, and A. Foux, *Effects of axial stretching on the resistivity of carbon black filled silicone rubber.* **23**(10): p. 567-571.
25. Hu, W., *Elastomeric transparent capacitive sensors based on an interpenetrating composite of silver nanowires and polyurethane: Applied Physics Letters: Vol 102, No 8.* Applied Physics Letters

2013. **102**(8).
26. Kim, K.K., *Highly Sensitive and Stretchable Multidimensional Strain Sensor with Prestrained Anisotropic Metal Nanowire Percolation Networks - Nano Letters (ACS Publications).* Nano Letters, 2015. **15**(8).
27. Heo, Y., *Secondary Sensitivity Control of Silver-Nanowire-Based Resistive-Type Strain Sensors by Geometric Modulation of the Elastomer Substrate - Heo - 2017 - Small - Wiley Online Library.* small, 2017.
28. Amjadi, M., et al., *Highly Stretchable and Sensitive Strain Sensor Based on Silver Nanowire–Elastomer Nanocomposite.* ACS Nano, 2014. **8**(5): p. 5154-5163.
29. Cheng, Y., et al., *Stretchable electronic skin based on silver nanowire composite fiber electrodes for sensing pressure, proximity, and multidirectional strain.* Nanoscale, 2017. **9**(11): p. 3834-3842.
30. Joo, Y., et al., *Silver nanowire-embedded PDMS with a multiscale structure for a highly sensitive and robust flexible pressure sensor.* Nanoscale, 2015. **7**(14): p. 6208-6215.
31. Xu, F. and Y. Zhu, *Highly Conductive and Stretchable Silver Nanowire Conductors.* Advanced Materials, 2012. **24**(37): p. 5117-5122.
32. Yao, S. and Y. Zhu, *Wearable multifunctional sensors using printed stretchable conductors made of silver nanowires.* Nanoscale, 2014. **6**(4): p. 2345-2352.
33. Yun, S., et al., *Compliant Silver Nanowire-Polymer Composite Electrodes for Bistable Large Strain Actuation.* Advanced Materials, 2012. **24**(10): p. 1321-1327.
34. Hu, W., et al., *Intrinsically stretchable transparent electrodes based on silver-nanowire–crosslinked-polyacrylate composites.* Nanotechnology, 2012. **23**(34): p. 344002.
35. Huang, G.-W., H.-M. Xiao, and S.-Y. Fu, *Wearable Electronics of Silver-Nanowire/Poly(dimethylsiloxane) Nanocomposite for Smart Clothing.* Scientific Reports, 2015. **5**.
36. Lee, H., et al., *Directly printed stretchable strain sensor based on ring and diamond shaped silver nanowire electrodes.* RSC Advances, 2015. **5**(36): p. 28379-28384.
37. Lee, S., et al., *Ag Nanowire Reinforced Highly Stretchable Conductive Fibers for Wearable Electronics.* Advanced Functional Materials, 2015. **25**(21): p. 3114-3121.
38. Ho, M.D., et al., *Percolating Network of Ultrathin Gold Nanowires and Silver Nanowires toward "Invisible" Wearable Sensors for Detecting Emotional Expression and Apexcardiogram.* Advanced Functional Materials, 2017. **27**(25): p. n/a-n/a.
39. De, S., et al., *Silver Nanowire Networks as Flexible, Transparent, Conducting Films: Extremely High DC to Optical Conductivity Ratios.* ACS Nano, 2009. **3**(7): p. 1767-1774.
40. Finn, D.J., M. Lotya, and J.N. Coleman, *Inkjet Printing of Silver Nanowire Networks.* ACS Applied Materials & Interfaces, 2015. **7**(17): p. 9254-9261.
41. Sorel, S., et al., *The dependence of the optoelectrical properties of silver nanowire networks on nanowire length and diameter.* Nanotechnology, 2012. **23**(18): p. 185201.
42. Lordi, V. and N. Yao, *Molecular mechanics of binding in carbon-nanotube-polymer composites.* Journal of Materials Research, 2000. **15**: p. 2770-2779.
43. Liao, K. and S. Li, *Interfacial characteristics of a carbon nanotube–polystyrene composite system.* Applied Physics Letters, 2001. **79**(25): p. 4225-4227.
44. Slobodian, P., P. Riha, and P. Saha, *A highly-deformable composite composed of an entangled network of electrically-conductive carbon-nanotubes embedded in elastic polyurethane.* Carbon, 2012. **50**(10): p. 3446-3453.

45. Kim, Y., et al., *Stretchable nanoparticle conductors with self-organized conductive pathways.* Nature, 2013. **500**(7460): p. 59-63.
46. Stauffer, D. and A. Aharony, *Introduction To Percolation Theory*. 1994: CRC Press. 205.
47. Cunningham, G., et al., *Percolation scaling in composites of exfoliated MoS2 filled with nanotubes and graphene.* Nanoscale, 2012. **4**(20): p. 6260-6264.
48. Garboczi, E.J., et al., *Geometrical percolation threshold of overlapping ellipsoids.* Physical Review E, 1995. **52**(1): p. 819-828.
49. Madaria, A.R., et al., *Uniform, highly conductive, and patterned transparent films of a percolating silver nanowire network on rigid and flexible substrates using a dry transfer technique.* Nano Research, 2010. **3**(8): p. 564-573.
50. Gelves, G.A. *Low Electrical Percolation Threshold of Silver and Copper Nanowires in Polystyrene Composites - Gelves - 2006 - Advanced Functional Materials - Wiley Online Library*. 2006 2016/04/06/13:25:46; Available from: http://onlinelibrary.wiley.com/doi/10.1002/adfm.200600336/full.
51. Fan, Q., et al., *The use of a carbon nanotube layer on a polyurethane multifilament substrate for monitoring strains as large as 400%.* Carbon, 2012. **50**(11): p. 4085-4092.
52. Yamada, T., et al., *A stretchable carbon nanotube strain sensor for human-motion detection.* Nature Nanotechnology, 2011. **6**(5): p. 296-301.
53. Fu, X.-W., et al., *Strain dependent resistance in chemical vapor deposition grown graphene.* Applied Physics Letters, 2011. **99**(21): p. 213107.
54. Li, X., et al., *Stretchable and highly sensitive graphene-on-polymer strain sensors.* Scientific Reports, 2012. **2**: p. srep00870.
55. Hu, W., et al., *Elastomeric transparent capacitive sensors based on an interpenetrating composite of silver nanowires and polyurethane.* Applied Physics Letters, 2013. **102**(8): p. 083303.
56. Kang, I., et al., *A carbon nanotube strain sensor for structural health monitoring.* Smart Materials and Structures, 2006. **15**(3): p. 737-748.
57. Gang, Y., et al., *A carbon nanotube/polymer strain sensor with linear and anti-symmetric piezoresistivity.* Journal of Composite Materials, 2011. **45**(12): p. 1315-1323.
58. Loh, K.J., et al., *Multifunctional layer-by-layer carbon nanotube–polyelectrolyte thin films for strain and corrosion sensing.* Smart Materials and Structures, 2007. **16**(2): p. 429.
59. Liu, X., C. Shi, and R. Chuai, *Polycrystalline Silicon Piezoresistive Nano Thin Film Technology.* Solid State Circuits Technologie, 2010.
60. Stadermann, M., et al., *Nanoscale study of conduction through carbon nanotube networks.* Physical Review B, 2004. **69**(20): p. 201402.